

Electronic Supporting Information

Strong Impact of Intramolecular Hydrogen Bonding on the Cathodic Path of [Re (3,3'-dihydroxy-2,2'-bipyridine)(CO)₃Cl] and Catalytic Reduction of Carbon Dioxide

James O. Taylor¹, Gaia Neri², Liam Banerji², Alexander J. Cowan² and František Hartl^{1*}

¹Department of Chemistry, University of Reading, Reading, England, RG6 6AD, United Kingdom

²Department of Chemistry, Stephenson Institute for Renewable Energy, University of Liverpool, L69 7ZF, United Kingdom

Corresponding Author

E-mail: f.hartl@reading.ac.uk

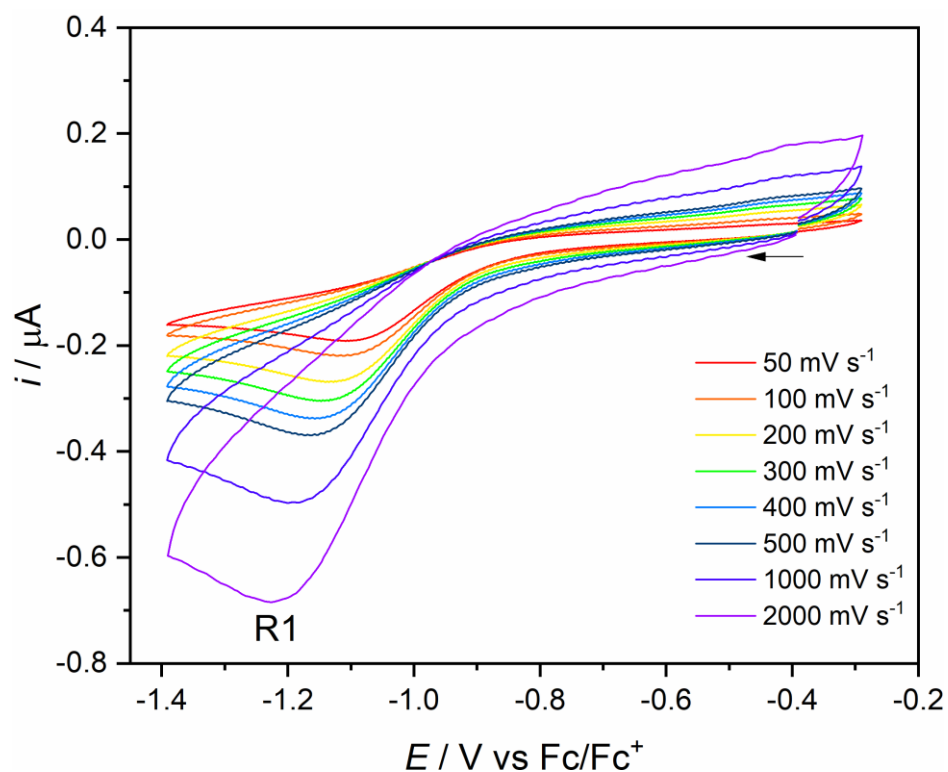


Figure S1: Cyclic voltammograms of $[\text{Re}(3,3'\text{-DHBPY})(\text{CO})_3\text{Cl}]$ in $\text{THF}/\text{Bu}_4\text{NPF}_6$ in the region of R1. Experimental conditions: Pt microdisc, $T = 298 \text{ K}$, scan rates $\nu = 50 - 2000 \text{ mV s}^{-1}$.

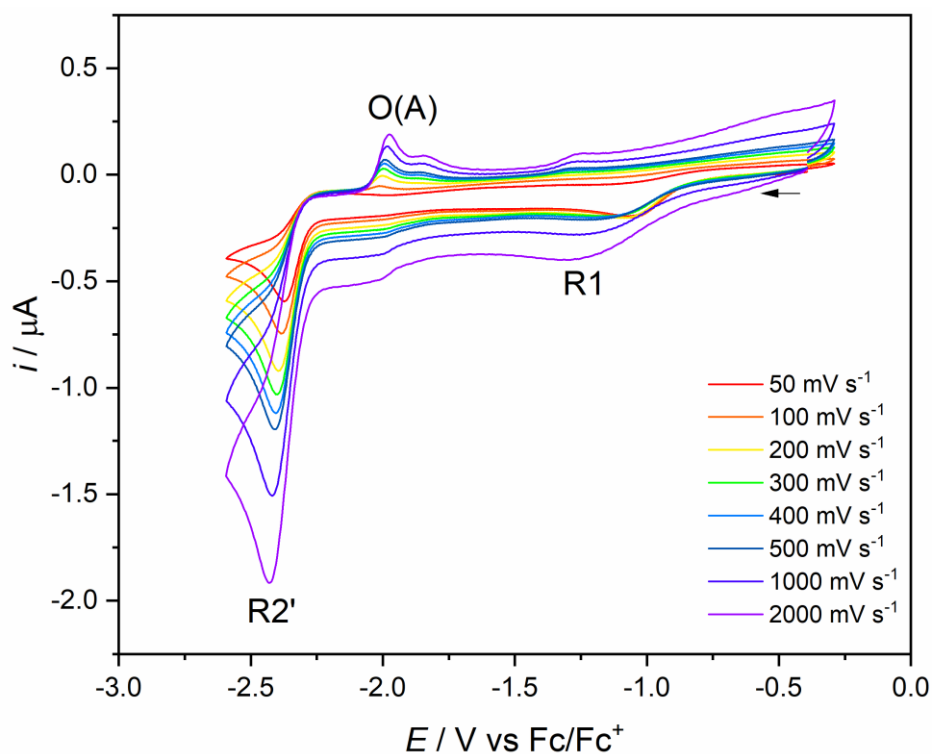


Figure S2: Cyclic voltammograms of $[\text{Re}(3,3'\text{-DHBPY})(\text{CO})_3\text{Cl}]$ in $\text{THF}/\text{Bu}_4\text{NPF}_6$ across the full cathodic region. Experimental conditions: Pt microdisc, $T = 298 \text{ K}$, scan rates $\nu = 50 - 2000 \text{ mV s}^{-1}$.

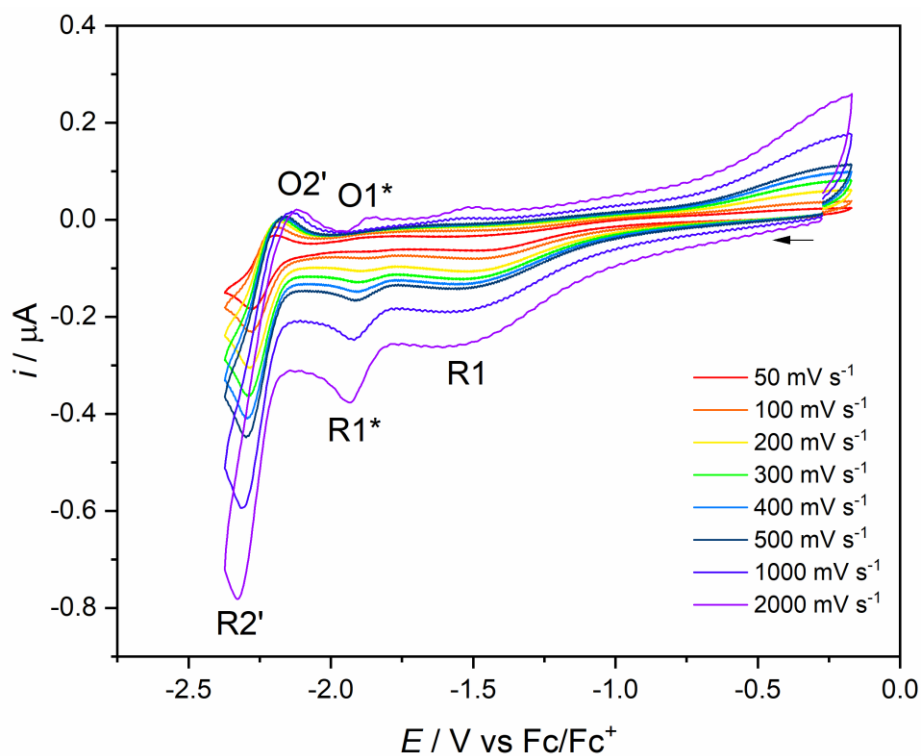


Figure S3: Cyclic voltammograms of $[\text{Re}(3,3'\text{-DHBPY})(\text{CO})_3\text{Cl}]$ in $\text{THF}/\text{Bu}_4\text{NPF}_6$ across the cathodic potential region. Experimental conditions: Pt microdisc, $T = 195 \text{ K}$, scan rates $\nu = 50 - 2000 \text{ mV s}^{-1}$.

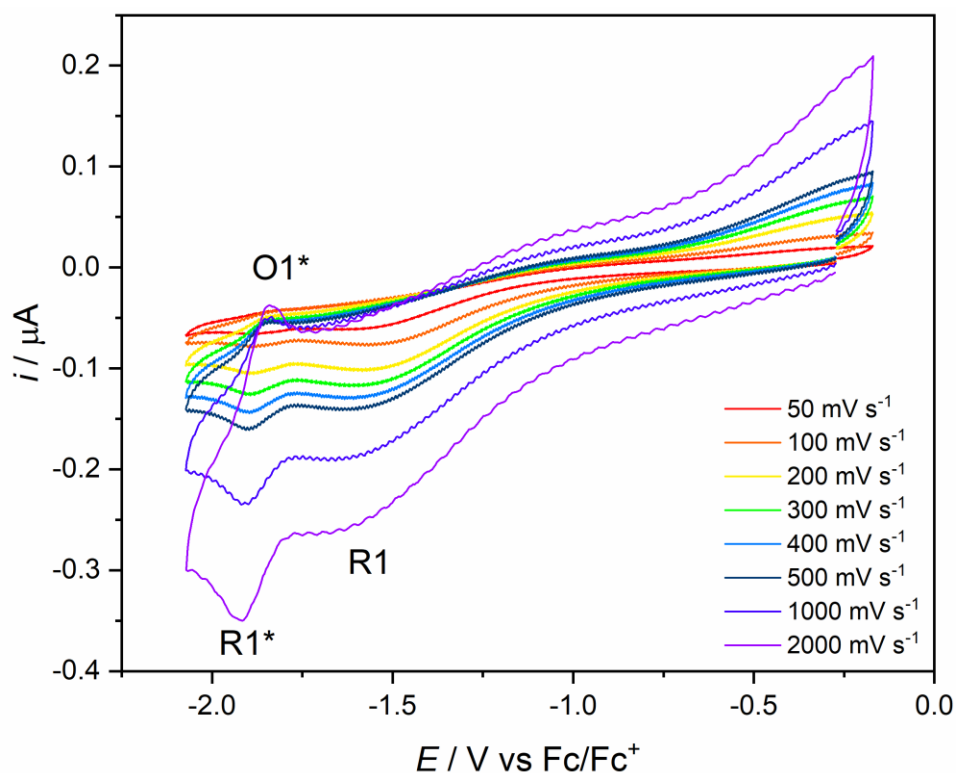


Figure S4: Cyclic voltammograms of $[\text{Re}(3,3'\text{-DHBPY})(\text{CO})_3\text{Cl}]$ in $\text{THF}/\text{Bu}_4\text{NPF}_6$ up to R1^* . Experimental conditions: Pt microdisc, $T = 195 \text{ K}$, scan rates $\nu = 50 - 2000 \text{ mV s}^{-1}$.

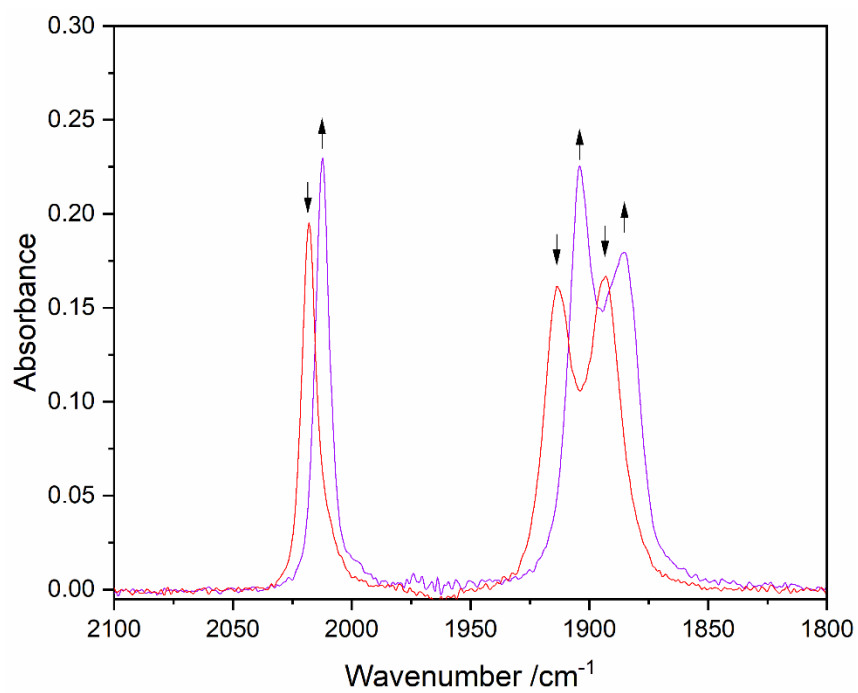


Figure S5. Chemical deprotonation of [Re(3,3'-DHBPY)(CO)₃Cl] to [Re(3,3'-DHBPY-H⁺)(CO)₃Cl]⁻ in THF caused by the addition of 1 equiv. NaHMDS.

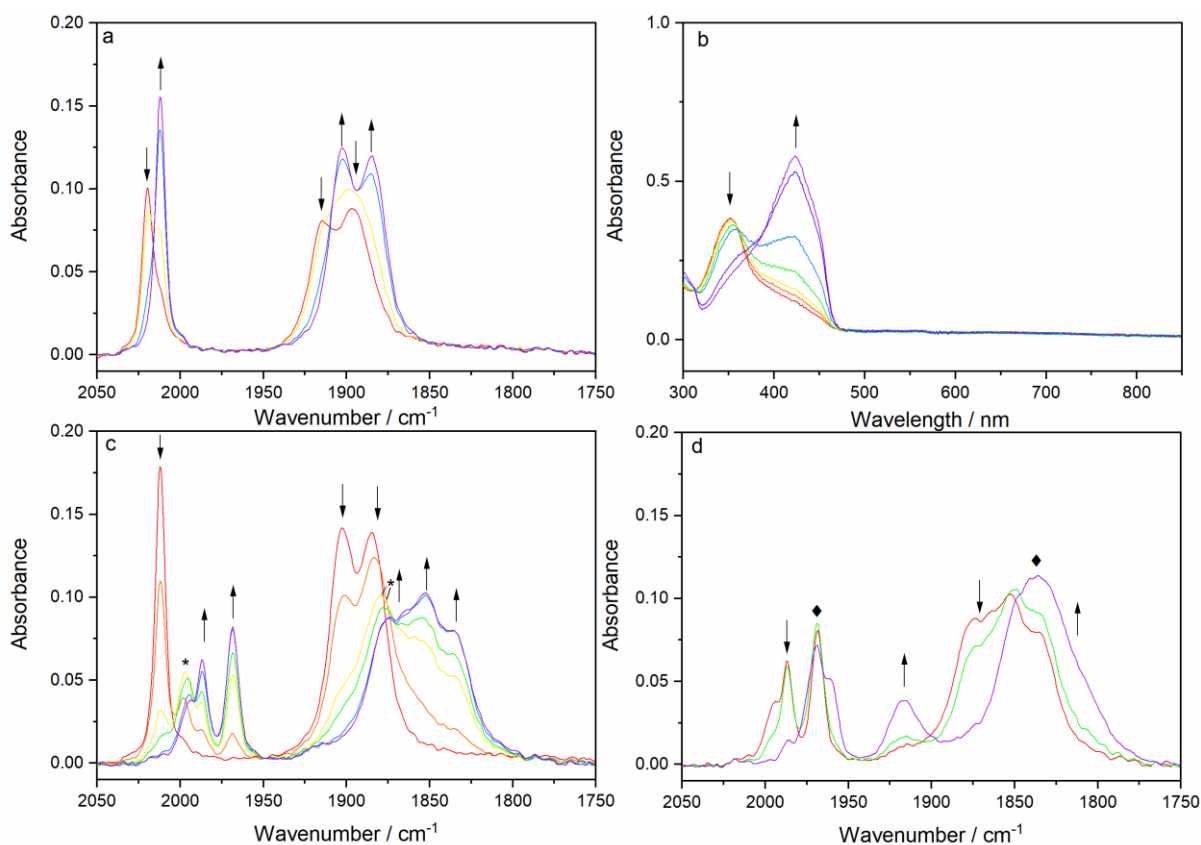


Figure S6. (a) IR and (b) UV-VIS spectroelectrochemistry of $[\text{Re}(3,3'\text{-DHBPY})(\text{CO})_3\text{Cl}]$ (\downarrow) in $\text{PrCN}/\text{Bu}_4\text{NPF}_6$ at 298 K as it is converted by reductive deprotonation at R1 to $[\text{Re}(3,3'\text{-DHBPY-H}^+)(\text{CO})_3\text{Cl}]^-$ (\uparrow) in an OTTE cell. (c) IR spectroelectrochemistry of $[\text{Re}(3,3'\text{-DHBPY-H}^+)(\text{CO})_3\text{Cl}]^-$ (\downarrow) as it undergoes, $1e^-$ reduction at the onset of R2' and ETC conversion to $[\text{Re}(3,3'\text{-DHBPY})(\text{CO})_3\text{Cl}]^-$ (*). The latter radical anion is further reduced on scanning through R2', forming the 6-coordinate redox couple $[\text{Re}(3,3'\text{-DHBPY-2H}^+)(\text{CO})_3(\text{PrCN})]^{n-}$ ($n = 2, 3$) (\uparrow) existing in redox equilibrium (cf. Figure 11). (d) $[\text{Re}(3,3'\text{-DHBPY-2H}^+)(\text{CO})_3(\text{PrCN})]^{2-}$ (\downarrow) continues to reduce by a small negative potential shift, generating mainly 5-coordinate $[\text{Re}(3,3'\text{-DHBPY-2H}^+)(\text{CO})_3]^{3-}$ (\uparrow) in equilibrium with 6-coordinate $[\text{Re}(3,3'\text{-DHBPY-2H}^+)(\text{CO})_3(\text{PrCN})]^{3-}$ (\blacklozenge).

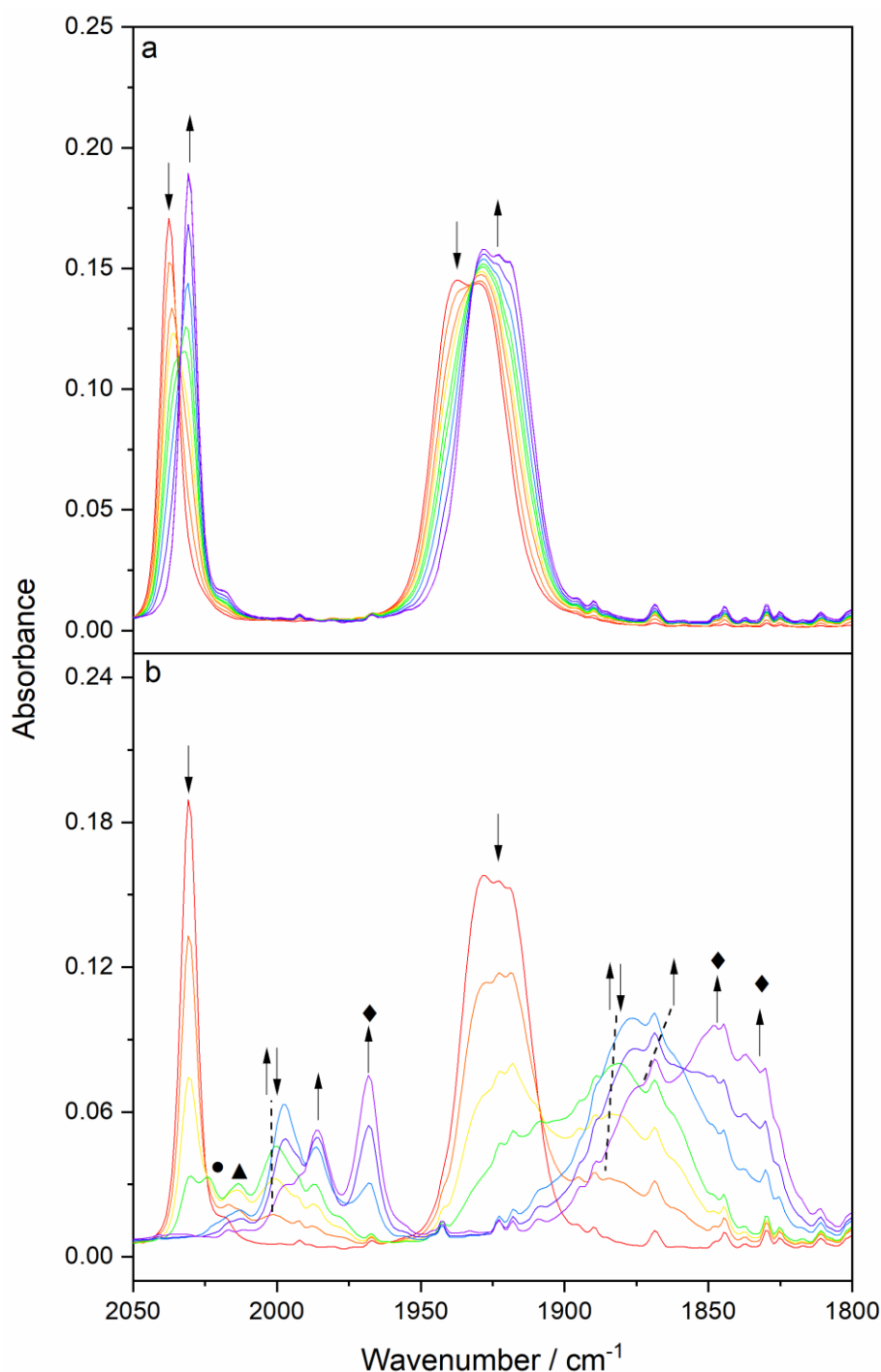


Figure S7. Cathodic IR spectroelectrochemistry of $[\text{Re}(3,3'\text{-DHBPY})(\text{CO})_3(\text{PrCN})]^+$ in $\text{PrCN}/\text{Bu}_4\text{NPF}_6$ at 223 K. (a) $1e^-$ reduction of the parent complex (\downarrow) at R1 producing deprotonated $[\text{Re}(3,3'\text{-DHBPY-H}^+)(\text{CO})_3(\text{PrCN})]$ (\uparrow). (b) Subsequent reduction of $[\text{Re}(3,3'\text{-DHBPY-H}^+)(\text{CO})_3(\text{PrCN})]$ (\downarrow) at R2' to give a mixture of products with dominating $[\text{Re}(3,3'\text{-DHBPY})(\text{CO})_3(\text{PrCN})]$ ($\uparrow\downarrow$) formed in an ETC step. The small band labelled with \bullet may belong to marginal reductively double-deprotonated $[\text{Re}(3,3'\text{-DHBPY-2H}^+)(\text{CO})_3(\text{PrCN})]^-$. Its $1e^-$ and $2e^-$ reduced forms, $[\text{Re}(3,3'\text{-DHBPY}^{2-}\text{-2H}^+)(\text{CO})_3(\text{PrCN})]^{2-}$ (\uparrow) and $[\text{Re}(3,3'\text{-DHBPY}^{2-}\text{-2H}^+)(\text{CO})_3(\text{PrCN})]^{3-}$ (\blacklozenge), terminate the cathodic path. The label \blacktriangle denotes an unassigned reduced intermediate (see also Figure 11b).

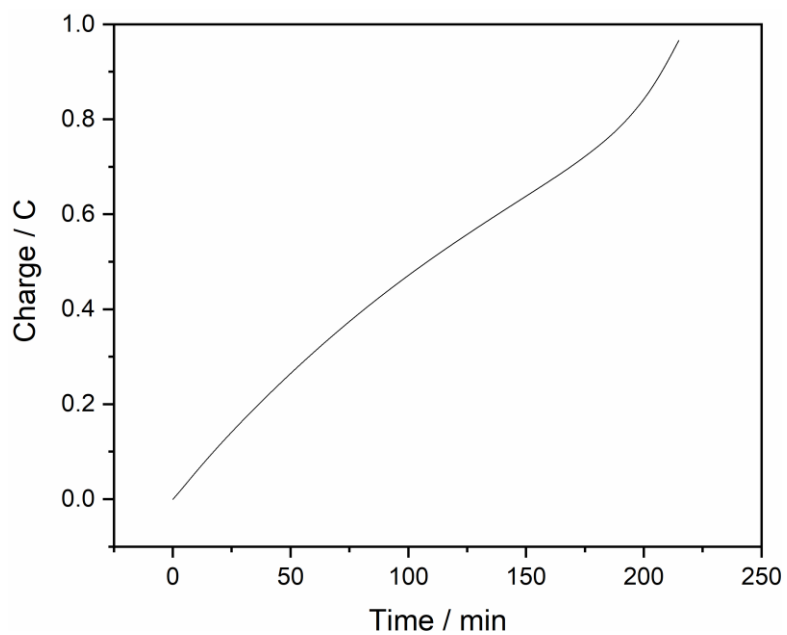


Figure S8. Charge vs time plot following the CPE of 3 mM $[\text{Re}(3,3'\text{-DHBPY})(\text{CO})_3\text{Cl}]$ in CO_2 -saturated 0.5 M THF/ Bu_4NPF_6 . The catalytic electrode potential was held at - 2.6 V vs Fc/Fc^+ for 3 h, using a Pt microdisc electrode (diameter of 2 mm).

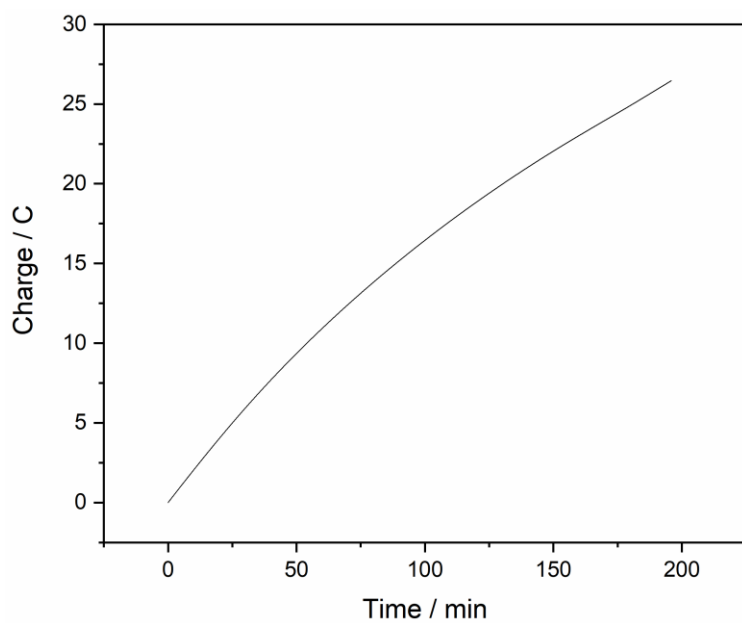


Figure S9. Charge vs time plot following the CPE of 3 mM $[\text{Re}(3,3'\text{-DHBPY})(\text{CO})_3\text{Cl}]$ in CO_2 -saturated 0.5 M THF/ Bu_4NPF_6 . The catalytic electrode potential was held at - 2.6 V vs Fc/Fc^+ for 3 h, using a Pt foil electrode (surface area of $2 \times 0.96 \text{ cm}^2$).

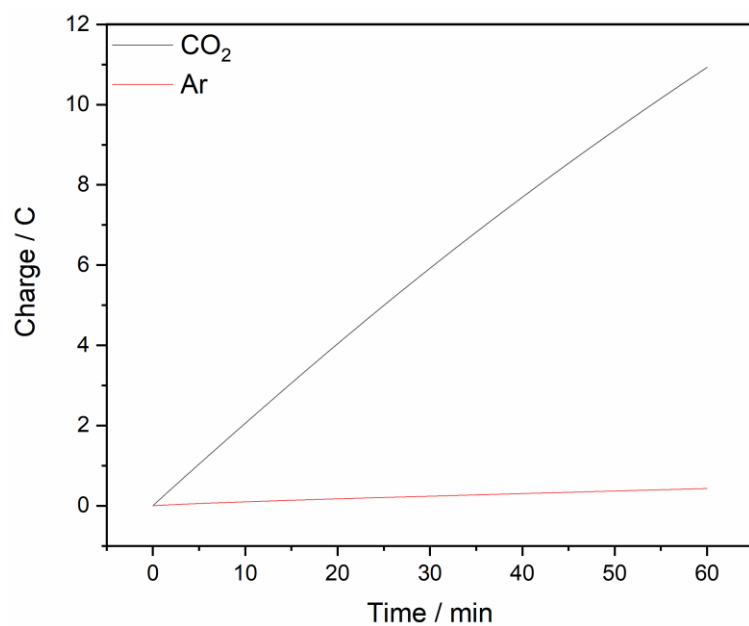


Figure S10. Charge vs time plot following the CPE of 3 mM [Re(3,3'-DHBPY)(CO)₃Cl] in CO₂-saturated (black) and Ar-saturated (red) 0.5 M THF/Bu₄NPF₆. The catalytic electrode potential was held at - 2.6 V vs Fc/Fc⁺ for 1 h, using a Pt foil electrode (surface area of 2 × 0.96 cm²).